Drug Delivery

International Edition: DOI: 10.1002/anie.201607303
German Edition: DOI: 10.1002/ange.201607303

# Mechanism-Guided Design and Synthesis of a Mitochondria-Targeting Artemisinin Analogue with Enhanced Anticancer Activity

*Chong-Jing Zhang[+], Jigang Wang[+],* Jianbin Zhang, Yew Mun Lee, Guangxue Feng, Teck Kwang Lim, Han-Ming Shen, Qingsong Lin,* and Bin Liu**

***Abstract:*** *Understanding the mechanism of action (MOA) of bioactive natural products will guide endeavor to improve their cellular activities. Artemisinin and its derivatives inhibit cancer cell proliferation, yet with much lower efficiencies than their roles in killing malaria parasites. To improve their efficacies on cancer cells, we studied the MOA of artemisinin using chemical proteomics and found that free heme could directly activate artemisinin. We then designed and synthesized a derivative, ART-TPP, which is capable of targeting the drug to mitochondria where free heme is synthesized. Remarkably, ART-TPP exerted more potent inhibition than its parent compound to cancer cells. A clickable probe ART-TPP-Alk was also employed to confirm that the attachment of the TPP group could label more mitochondrial proteins than that for the ART derivative without TPP (AP1). This work shows the importance of MOA study, which enables us to optimize the design of natural drug analogues to improve their biological activities.*

Artemisinin (ART) is a sesquiterpene lactone endoperoxide compound isolated from an annual wormwood (*Artemisia annua L.*). It potently kills malaria parasites, saving millions of lives.[1,2] Four decades after its discovery, the ART-based combination therapies (ACTs) remain the first line treatment for malaria as recommended by the World Health Organization (WHO).[3,4] Interestingly, recent studies suggested that ART may possess anticancer properties.[5–7] However, the majority of the reported ART analogues showed only limited potency in certain tumor cell lines.[8] Since understanding the mode of action (MOA) for drugs could contribute greatly towards the improvement of their cellular activities,[9–12] we seek to elucidate the MOA of ART, with the hope to find an effective strategy to improve the potency of ART against cancer cells.

ART contains a unique endoperoxide bridge (R-O-O-R′), which is crucial for its inhibitory activities.[13–15] It is widely accepted that the activation and breaking of endoperoxide bridge in solution leads to the generation of oxygen radicals, followed by its rearrangement to produce carbon radicals.[15] However, there remain debates over the exact mechanism of endoperoxide bridge activation in vivo.[16] Both free ferrous iron[17,18] and heme[19] have been proposed to be ART activators.[20] Very recently, we used a chemical proteomics approach to show that, heme, rather than free ferrous iron, directly activates ART in malaria parasites, which then promiscuously targets various proteins within the parasites.[21] Based on this discovery, we used alkyne-tagged ART probe AP1 in our current study (Figure 1 A), and with the help of the chemical proteomics approach, we demonstrate that ART is also activated by heme and it promiscuously targets multiple proteins to kill cancer cells. Moreover, we also find out that modulating the level of heme could greatly affect the anticancer activities of ART.

In human cells, fresh free heme is synthesized in the mitochondria.[22] Therefore, we hypothesize that by directing ART into mitochondria, we could potentially increase its anticancer activities. To confirm this hypothesis, we synthesized two ART analogues: ART-triphenylphosphoniumbromide (ART-TPP) and ART-TPP-alkyne (ART-TPP-Alk; Figure 1 A). TPP is a typical cation, which could direct molecules into mitochondria and this approach is more favorable in cancer cells than normal cells.[23,24] Indeed, our results demonstrate that ART-TPP could remarkably improve the anticancer activities of ART, while ART-TPP-Alk further validates that the TPP group could efficiently direct ART into mitochondria thus increase the activation level of ART and target more protein targets, which is further evidenced by chemical proteomics studies. Our study highlights the importance of MOA study in improving the biological activities of natural products.

Moving into the details of our study, the AP1 probe retains the core structure and activity of ART.[21] With this probe, we adopted a chemical proteomics approach to study the activation level of AP1 as illustrated in Figure 1 B. Briefly, AP1 was incubated with live cells or cell lysate before

[*] Dr. C. Zhang,[+] G. Feng, Prof. Dr. B. Liu
Department of Chemical and Biomolecular Engineering
National University of Singapore
4 Engineering Drive 4, Singapore, 117585 (Singapore)
E-mail: cheliub@nus.edu.sg
Dr. J. Wang[+]
The State Key Laboratory of Pharmaceutical Biotechnology
College of Life Science, Nanjing University
Nanjing, 210023 (China)
E-mail: wangjg@nju.edu.cn
Dr. J. Wang,[+] Y. M. Lee, T. K. Lim, Dr. Q. Lin
Department of Biological Science, National University of Singapore
14 Science Drive 4, Singapore 117543 (Singapore)
E-mail: dbslinqs@nus.edu.sg
Dr. J. Zhang, Prof. Dr. H. M. Shen
Department of Physiology, Yong Loo Lin School of Medicine
National University of Singapore
2 Medical Drive, Singapore, 117597 (Singapore)
Prof. Dr. B. Liu
Institute of Materials Research and Engineering
2 Fusionopolis Way, Singapore, 138634 (Singapore)
[+] These authors contributed equally to this work.
Supporting information and the ORCID identification number(s) for the author(s) of this article can be found under: http://dx.doi.org/10.1002/anie.201607303.

  

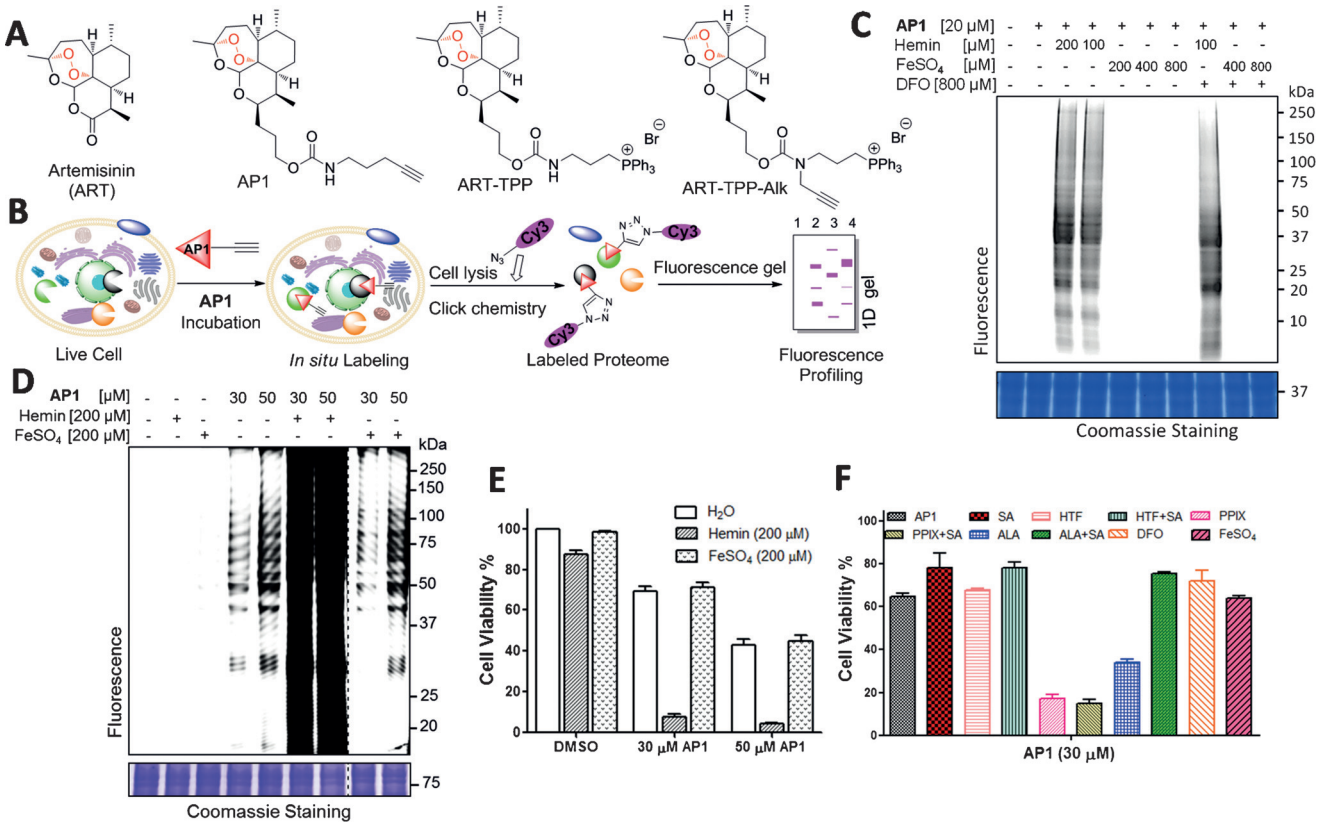


***Figure 1.*** A) Structures of artemisinin and probes used in this study; B) general workflow of the chemical proteomics approach with AP1; C) AP1 labeling profile in HCT116 cell lysate in the presence of different mediators; D) AP1 labeling profile in HCT116 live cells treated with or without hemin and $FeSO_4$; E) cell viability of HCT116 cells treated by AP1 with or without hemin and $FeSO_4$; F) cell viability of HCT116 cells treated by AP1 alone or AP1 with various mediators in the heme biosynthesis.

applying click chemistry to attach a fluorescent dye. This process allowed the fluorescence labelling of AP1 that had attached to their target proteins. The labeled proteins were then resolved with SDS-PAGE. Higher intensity of fluorescent bands in the SDS-PAGE gel indicates a higher activation level of AP1, hence increasing number of target proteins are bound by activated AP1.

To elucidate the activation mechanism of ART via this chemical proteomics approach, we first applied AP1 to label the cell lysate of cancer cells. As shown in Figure 1 C, the AP1 probe itself without any ART activator cannot label any proteins. We then used hemin as the source of heme to test for ART activation. Hemin is the oxidized form of heme, and it is stable in air for convenient use. The $Fe^{3+}$ in hemin has no ability to reduce endoperoxide double bond in ART. However, hemin can be easily reduced to heme in the presence of various reducing agents exist in the cells.[16,21,25–28] As shown in Figure 1 C, the addition of hemin to the cell lysate leads to sufficient protein labelling, which indicates that the source of heme is essential in activation of ART. In contrast, AP1 has negligible binding to any protein from the cell lysate in the presence of $FeSO_4$, even at a high concentration. Moreover, the addition of deferoxamine (DFO), a free-iron chelator, has no obvious effect on AP1 labeling of proteins in the presence of heme. Therefore, addition or depletion of ferrous iron in cell lysate has no obvious effect on activation of AP1. Subsequently, AP1 was applied to treat the live cells. AP1 labeled large amount of proteins when the cells were treated with hemin, which could be quickly converted into heme in the cellular environment.[26] Whereas in $FeSO_4$-treated cells AP1 could only label a small amount of proteins, at a level comparable to the cells without treatment (Figure 1 D). Collectively, both results from cell lysate and live cells indicate that free heme could effectively activate ART, while free ferrous iron has minimal effects on the activation of ART.

With a larger amount of activated ART, more cellular proteins could be targeted by ART, which could lead to enhanced anticancer activities. To confirm this hypothesis, we went on to examine the viability of HCT116 colorectal cancer cells treated with AP1, with the addition of hemin or $FeSO_4$. As shown in Figure 1 E, hemin or $FeSO_4$ alone has little effect on the viability of HCT116, and AP1 alone could only kill about 30 % of the cells after 24 hours of incubation. Similar to our AP1 binding results, addition of 200 μM of $FeSO_4$ did not increase the anticancer activities of AP1. Contrastingly, AP1 together with hemin could kill more than 90 % of the HCT116 cells. This is positively correlated with the amount of activated ART (Figure 1 D). The increased ART activation level leads to the marked decrease of the viability of HCT116 cells (Figure 1 E). Our results highlight that the addition of hemin, which is reduced to heme in vivo, could dramatically enhance

  

the cell killing effect of AP1 by increasing the amount of activated ART.

After confirming that an external source of heme could increase anticancer activity of the drug, we reasoned that the modulation of endogenous heme could also affect anticancer activity of ART. Synthesis of endogenous heme involves multiple steps, and there are a lot of intermediates and mediators that could modulate endogenous heme level (Figure 2B). As both δ-aminolevulinic acid (ALA) and protoporphyrin IX (PPIX) are intermediates of heme bio-

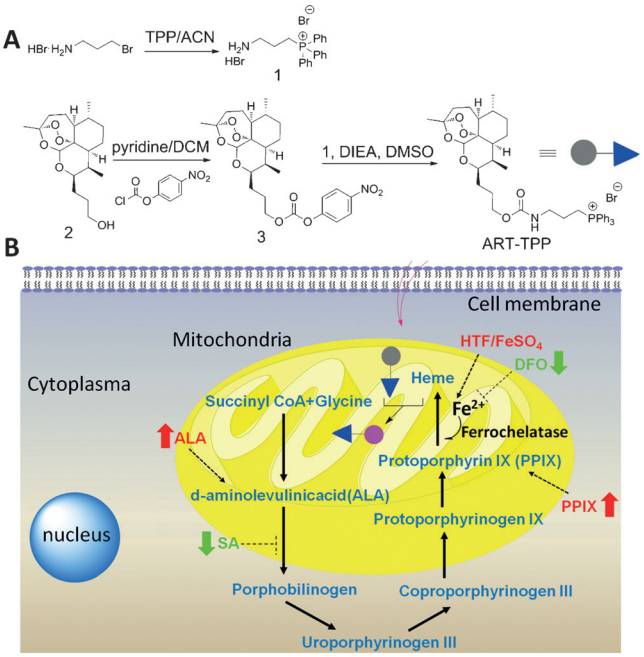


***Figure 2.*** A) Synthesis of ART-TPP; B) illustration of ART-TPP targeting mitochondria and its activation by heme.

synthesis, the addition of these two compounds could increase endogenous heme level. As expected, addition of ALA and PPIX increases the anticancer effect of ART (Figure 1F). On the other hand, succinylacetone (SA) is an inhibitor for the synthesis of porphobilinogen from ALA. Addition of SA decreases the anticancer activities of ART and even blocks the synergetic effects between ALA and ART, while PPIX could subvert the inhibitory effects of SA (Figure 1F). Co-administration of ART and DFO can apparently inhibit ART-induced cytotoxicity (Figure 1F). The partial inhibitory effect of DFO might be due to iron chelation that inhibits iron-related oxidative stress and sequesters the iron required for heme synthesis in cancer cells.[7,15,17,29–33] Furthermore, co-incubation of ART with human Holo Transferrin (HTF) or $FeSO_4$ did not have apparent effect on the cytotoxicity of ART(Figure 1F). This can be explained by the fact that the formation of ALA is the rate-limiting step of heme synthesis.[34] Since ALA is the substrate found upstream of the heme synthesis pathway, the production of the downstrem product PPIX in the heme synthesis pathway is dependent on the level of ALA. Therefore, by adding more exogenous iron to cancer cells that already possess a high intracellular iron concentration, it is less likely that the exogenous iron would affect the rates of heme production, since the generation of heme involves the incorporation of $Fe^{II}$ with PPIX, which in turn is greatly dependent on the amount of ALA.

Taken together, our chemical proteomics and cell viability experiments indicate that heme plays a decisive role on the activation of ART in cancer cells. However, intracellular free heme could promote the generation of reactive oxygen species to cause lipid peroxidation. This would subsequently induce membrane injury and yield cell apoptosis. As a consequence, the intracellular level of free heme is tightly controlled to be less than 100 nM within normal cells and the majority of heme is bound to carrier proteins.[35] As heme–protein complexes possess much lower ability to activate ART than free heme,[15] the intracellular location of free heme accessible to ART is vital for its anticancer activities.[33] Since the final step of heme biosynthesis occurs in mitochondria, we hypothesize that directing ART to the mitochondria could potentially increase the activation level of ART, yielding higher anticancer activities.

To confirm this hypothesis, we went on to synthesize the ART-TPP probe as shown in Figure 2A. In brief, the compound 3-bromopropylamine hydrobromide was reacted with triphenylphosphine to give the key intermediate 1. Subsequently, 1 was reacted with activated ART to generate ART-TPP (Supporting Information, Figure S1–S8) with an overall yield of 10.4%. With ART-TPP at hand, we first compared its cytotoxicity with ART using various cell lines. As shown in Figure 3, ART-TPP is cytotoxic to all tested cancer cells, with the $IC_{50}$ values of 2.84 μM for MDA-MB-231 cells, 0.82 μM for HeLa cells, 6.13 μM for SKBR3 cells, and 1.73 μM for HCT116 cells. In comparison, the cytotoxicity of ART-TPP is 26-fold and 94-fold more potent than ART in MDA-MB-231 and HeLa cells, respectively. Moreover, little cytotoxicity in HCT116 cells was observed for compound 1 containing only the TPP group without ART (Figure 3A), which verifies the important synergetic effects between TPP group and ART in enhancing its anticancer activities.

Next, to confirm that ART-TPP is distributed to the mitochondria, we measured the mitochondrial membrane

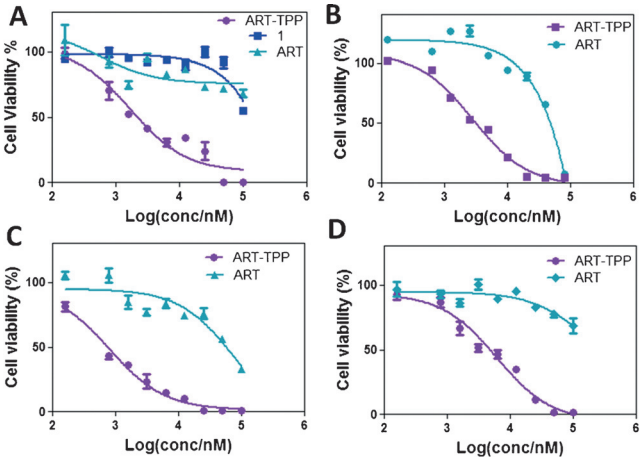


***Figure 3.*** Cell viabilities A) of HCT116, B) MDA-MB-231, C) HeLa, and D) SKBR3 treated with ART, ART-TPP or 1.

  

potential (MMP) using a fluorescent marker of tetramethylrhodamine ethyl ester (TMRE). TMRE is very emissive when MMP is high.[35,36] As shown in the Supporting Information, Figure S11, cells treated with DMSO or ART possess high MMP as reflected by the high fluorescent signals. No fluorescence was detected for the cells treated with ART-TPP under the same condition, suggesting that the probe was distributed into the mitochondria, thus reducing the MMP.

Subsequently, to directly visualize the cellular distribution of ART-TPP and perform critical proteomics study, we went on to synthesize a clickable probe (ART-TPP-Alk) to allow for the attachment of a fluorescent molecule and biotin tag through click chemistry. The probe was synthesized as shown in Figure 4A. Briefly, the propargyl bromide was reacted with compound **1** to generate compound **3**. Compound **3** was then reacted with activated ART to yield the ART-TPP-Alk probe. ART-TPP-Alk possesses similar cytotoxic activity with ART-TPP (Supporting Information, Figure S12A), illustrating that the attachment of an alkyne tag has little effect on its overall biological activity while allowing us to visualize and identify the cellular targets of ART-TPP. The images shown in the Supporting Information, Figures S12B–E reveal that the fluorescent signal from the ART-TPP-Alk overlaps well with that from the mitochondria tracker, demonstrating that majority of the probe indeed localizes well in the mitochondria after cellular uptake.

Finally, we studied the effects of the TPP group on protein labeling profile. Both AP1 and ART-TPP-Alk were used to treat live cells. The labeled proteins were clicked with rhodamine azide and resolved by SDS-PAGE. Compared with AP1, ART-TPP-Alk is able to label more proteins (Figure 4B). Furthermore, pre-incubation of excess ART or ART-TPP in cell lysate remarkably decreases the protein labeling of both AP1 and ART-TPP-Alk (Supporting Information, Figure S13), suggesting that they bind to similar protein targets as their parent. Next, we proceeded to identify the covalent binding targets of AP1 and ART-TPP-Alk in HeLa cells. As shown in the Supporting Information, Tables S1–S4, AP1 and ART-TPP-Alk covalently modified 321 and 860 proteins, respectively, which is consistent with the labeling profile shown in SDS-PAGE (Figure 4B). More importantly, AP1 is able to bind to 76 proteins from the mitochondria, while ART-TPP-Alk is able to bind to 209 proteins from the mitochondria (Figure 4C). Furthermore, most of the proteins labeled by ART-TPP-Alk have higher scores than those labeled by AP1 (Figure 4D). A protein with a higher score reflects the larger abundance of its unique peptides identified during MS analysis. Therefore, these results suggest that there are more activated ART-TPP-Alk to bind to target proteins. As mitochondria is the powerhouse of the cell, the fact that more mitochondria proteins are covalently modified by ART-TPP-Alk inevitably make it more potent than ART.

In conclusion, we have elucidated the MOA of the natural product ART using the chemical proteomics approach in cancer cells. Our results validate that free heme is the main activator in cancer cells. Guided by this unique MOA, we designed and synthesized ART-TPP, where the TPP group could direct ART to the mitochondria. We showed that the incorporation of this mitochondria targeting moiety could remarkably increase the anticancer activities of ART. The fluorescence imaging results also confirmed that the TPP group could efficiently direct ART-TPP into the mitochondria, leading to the reduction of MMP. More importantly, the proteomics results revealed that ART-TPP-Alk could label more proteins in mitochondria than AP1 did. The more protein targets and higher scores identified with ART-TPP-Alk also suggest its greater activation and higher potency than AP1. As such, our results highlight that the activity optimization of natural products could benefit from MOA studies. As cancer cells were reported to possess higher MMP than normal cells, TPP could selectively target the probe to cancer cells to a certain extent.[36–38] Moreover, cancer cells are also reported to have higher heme level than normal cells.[39,40] Taken together, the concentration and activation level of ART-TPP are expected to be higher in cancer cells than in normal cells. Thus, we anticipate that ART-TPP could have good performance in animal cancer models, which is our next goal of study.

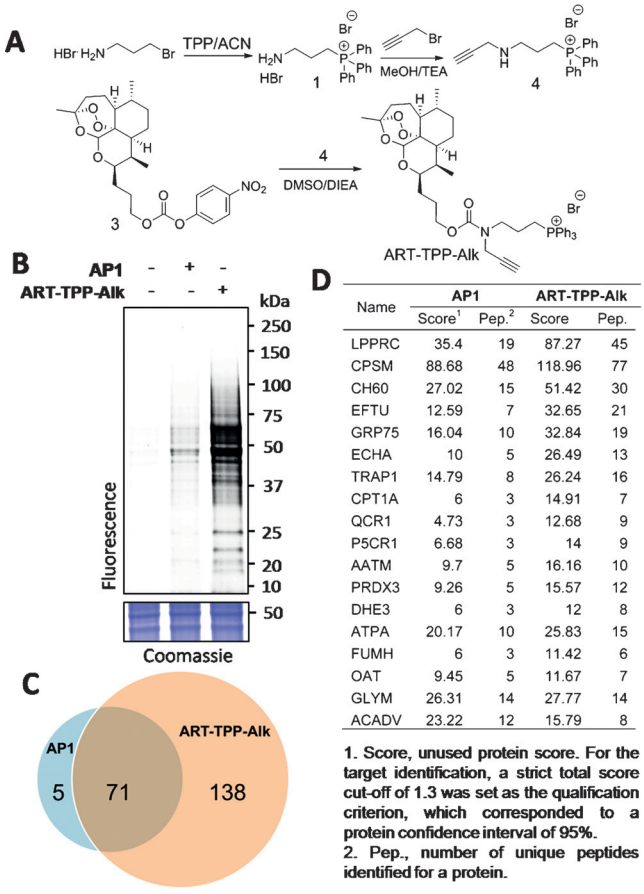


D

| Name | AP1 | | ART-TPP-Alk | |
|---|---|---|---|---|
| | Score[1] | Pep.[2] | Score | Pep. |
| LPPRC | 35.4 | 19 | 87.27 | 45 |
| CPSM | 88.68 | 48 | 118.96 | 77 |
| CH60 | 27.02 | 15 | 51.42 | 30 |
| EFTU | 12.59 | 7 | 32.65 | 21 |
| GRP75 | 16.04 | 10 | 32.84 | 19 |
| ECHA | 10 | 5 | 26.49 | 13 |
| TRAP1 | 14.79 | 8 | 26.24 | 16 |
| CPT1A | 6 | 3 | 14.91 | 7 |
| QCR1 | 4.73 | 3 | 12.68 | 9 |
| P5CR1 | 6.68 | 3 | 14 | 9 |
| AATM | 9.7 | 5 | 16.16 | 10 |
| PRDX3 | 9.26 | 5 | 15.57 | 12 |
| DHE3 | 6 | 3 | 12 | 8 |
| ATPA | 20.17 | 10 | 25.83 | 15 |
| FUMH | 6 | 3 | 11.42 | 6 |
| OAT | 9.45 | 5 | 11.67 | 7 |
| GLYM | 26.31 | 14 | 27.77 | 14 |
| ACADV | 23.22 | 12 | 15.79 | 8 |

1. Score, unused protein score. For the target identification, a strict total score cut-off of 1.3 was set as the qualification criterion, which corresponded to a protein confidence interval of 95%.
2. Pep., number of unique peptides identified for a protein.

***Figure 4.*** A) Synthesis of ART-TPP-Alk; B) labeling profile in HeLa live cells treated with AP1 (20 μM) or ART-TPP-Alk (20 μM); C) number of labeled proteins locating in mitochondria for AP1 and ART-TPP-Alk; D) comparison of selected proteins labeled by both AP1 and ART-TPP-Alk.

## Acknowledgements

We thank the Singapore NRF Investigatorship (R279-000-444-281 and R279-000-483-281), National University of Singapore (R279-000-482-133), and the Institute of Materials Research and Engineering of Singapore (IMRE/14-8P1110) for financial support.

**Keywords:** anticancer activity · drug delivery · fluorescent probe · mitochondria targeting · triphenylphosphonium

**How to cite:** *Angew. Chem. Int. Ed.* **2016**, *55*, 13770–13774
*Angew. Chem.* **2016**, *128*, 13974–13978

[1] Y. Tu, *Nat. Med.* **2011**, *17*, 1217–1220.
[2] Y. Tu, *Angew. Chem. Int. Ed.* **2016**, *55*, 10210; *Angew. Chem.* **2016**, *128*, 10366.
[3] N. J. White, *Lancet* **2014**, *383*, 1439–1440.
[4] B. Greenwood, *N. Engl. J. Med.* **2014**, *371*, 474–475.
[5] L. Y. Kong, R. X. Tan, *Nat. Prod. Rep.* **2015**, *32*, 1617–1621.
[6] A. Hamacher-Brady, H. A. Stein, S. Turschner, I. Toegel, R. Mora, N. Jennewein, T. Efferth, R. Eils, N. R. Brady, *J. Biol. Chem.* **2011**, *286*, 6587–6601.
[7] N.-D. Yang, S.-H. Tan, S. Ng, Y. Shi, J. Zhou, K. S. W. Tan, W.-S. F. Wong, H.-M. Shen, *J. Biol. Chem.* **2014**, *289*, 33425–33441.
[8] W. E. Ho, H. Y. Peh, T. K. Chan, W. S. F. Wong, *Pharmacol. Ther.* **2014**, *142*, 126–139.
[9] S. Ziegler, V. Pries, C. Hedberg, H. Waldmann, *Angew. Chem. Int. Ed.* **2013**, *52*, 2744–2792; *Angew. Chem.* **2013**, *125*, 2808–2859.
[10] T. Böttcher, M. Pitscheider, S. A. Sieber, *Angew. Chem. Int. Ed.* **2010**, *49*, 2680–2698; *Angew. Chem.* **2010**, *122*, 2740–2759.
[11] J. Wang, L. Gao, Y. M. Lee, K. A. Kalesh, Y. S. Ong, J. Lim, J.-E. Jee, H. Sun, S. S. Lee, Z.-C. Hua, et al., *Pharmacol. Ther.* **2016**, DOI: 10.1016/j.pharmthera.2016.01.010.
[12] J. Wang, X. F. Tan, V. S. Nguyen, P. Yang, J. Zhou, M. Gao, Z. Li, T. K. Lim, Y. He, C. S. Ong, et al., *Mol. Cell. Proteomics* **2014**, *13*, 876–886.
[13] S. Krishna, L. Bustamante, R. K. Haynes, H. M. Staines, *Trends Pharmacol. Sci.* **2008**, *29*, 520–527.
[14] X. C. Ding, H. P. Beck, G. Raso, *Trends Parasitol.* **2011**, *27*, 73–81.
[15] P. M. O'Neill, V. E. Barton, S. A. Ward, *Molecules* **2010**, *15*, 1705–1721.
[16] B. Meunier, A. Robert, *Acc. Chem. Res.* **2010**, *43*, 1444–1451.
[17] P. A. Stocks, P. G. Bray, V. E. Barton, M. Al-Helal, M. Jones, N. C. Araujo, P. Gibbons, S. A. Ward, R. H. Hughes, G. A. Biagini, et al., *Angew. Chem. Int. Ed.* **2007**, *46*, 6278–6283; *Angew. Chem.* **2007**, *119*, 6394–6399.
[18] U. Eckstein-Ludwig, R. J. Webb, I. D. A. van Goethem, J. M. East, A. G. Lee, M. Kimura, P. M. O'Neill, P. G. Bray, S. A. Ward, S. Krishna, *Nature* **2003**, *424*, 957–961.
[19] S. R. Meshnick, *Int. J. Parasitol.* **2002**, *32*, 1655–1660.
[20] N. Klonis, D. J. Creek, L. Tilley, *Curr. Opin. Microbiol.* **2013**, *16*, 722–727.
[21] J. Wang, C.-J. Zhang, W. N. Chia, C. C. Y. Loh, Z. Li, Y. M. Lee, Y. He, L.-X. Yuan, T. K. Lim, M. Liu, et al., *Nat. Commun.* **2015**, *6*, 10111.
[22] P. Ponka, *Am. J. Med. Sci.* **1999**, *318*, 241–256.
[23] L. F. Yousif, K. M. Stewart, S. O. Kelley, *ChemBioChem* **2009**, *10*, 1939–1950.
[24] R. A. J. Smith, R. C. Hartley, M. P. Murphy, *Antioxid. Redox Signaling* **2011**, *15*, 3021–3038.
[25] Y. Zhou, W. Li, Y. Xiao, *ACS Chem. Biol.* **2016**, DOI: acschembio.5b01043.
[26] J. L. Granick, S. Sassa, *J. Biol. Chem.* **1978**, *253*, 5402–5406.
[27] M. Rodriguez, C. Claparols, A. Robert, B. Meunier, *ChemBioChem* **2002**, *3*, 1147–1149.
[28] Y. Ying-Zi, W. Asawamahasakda, S. R. Meshnick, *Biochem. Pharmacol.* **1993**, *46*, 336–339.
[29] B. J. Reeder, M. T. Wilson, *Chem. Res. Toxicol.* **2005**, *18*, 1004–1011.
[30] B. J. Reeder, R. C. Hider, M. T. Wilson, *Free Radical Biol. Med.* **2008**, *44*, 264–273.
[31] T. Antoine, N. Fisher, R. Amewu, P. M. O'Neill, S. A. Ward, G. A. Biagini, *J. Antimicrob. Chemother.* **2014**, *69*, 1005–1016.
[32] S. G. Sullivan, E. Baysal, a. Stern, *Biochim. Biophys. Acta Biomembr.* **1992**, *1104*, 38–44.
[33] I. Morel, J. Cillard, G. Lescoat, O. Sergent, N. Pasdeloup, A. Z. Ocaktan, M. A. Abdallah, P. Brissot, P. Cillard, *Free Radical Biol. Med.* **1992**, *13*, 499–508.
[34] A. S. Tsiftsoglou, A. I. Tsamadou, L. C. Papadopoulou, *Pharmacol. Ther.* **2006**, *111*, 327–345.
[35] A. A. Khan, J. G. Quigley, *Biochim. Biophys. Acta Mol. Cell Res.* **2011**, *1813*, 668–682.
[36] F. Wang, M. A. Ogasawara, P. Huang, *Mol. Aspects Med.* **2010**, *31*, 75–92.
[37] S. Davis, M. J. Weiss, J. R. Wong, T. J. Lampidis, L. B. Chen, *J. Biol. Chem.* **1985**, *260*, 13844–13850.
[38] Q. Hu, M. Gao, G. Feng, B. Liu, *Angew. Chem. Int. Ed.* **2014**, *53*, 14225–14229; *Angew. Chem.* **2014**, *126*, 14449–14453.
[39] J. Hooda, D. Cadinu, M. M. Alam, A. Shah, T. M. Cao, L. A. Sullivan, R. Brekken, L. Zhang, *PLoS One* **2013**, *8*, DOI: 10.1371/journal.pone.0063402.
[40] W. Ye, L. Zhang, *Biochem. Biophys. Res. Commun.* **2004**, *315*, 546–554.

Received: July 28, 2016
Published online: October 6, 2016

  